Rate constants for deactivation of $N_2(A\ ^3\Sigma_u^+, v'=0,1)$ by O

L. G. Piper and G. E. Caledonia

Physical Sciences Inc., Woburn, Massachusetts 01801

J. P. Kennealy

Air Force Geophysics Laboratories, Bedford, Massachusetts 01730
(Received 9 March 1981; accepted 26 May 1981)

The removal of $N_2(A\ ^3\Sigma_u^+, v'=0,1)$ by O has been studied in a room temperature discharge–flow apparatus by monitoring the temporal decay of the 0,6 and 1,10 bands of the Vegard–Kaplan system. The measured rate constants are (2.8 ± 0.4) and $(3.4\pm0.6)\times10^{-11}$ cm^3 molecule^{-1} s^{-1} for $v'=0$ and 1, respectively.

I. INTRODUCTION

It has been suggested that the reactions of N_2 $(A^3\Sigma_u^+)$ with atomic and molecular oxygen could be significant sources of odd nitrogen and vibrationally excited NO in the upper atmosphere.[1] For the interaction between $N_2(A)$ and atomic oxygen, the possible reaction channels are as follows:

$$N_2(A\ ^3\Sigma_u^+)_{v'=0} + O(^3P) \rightarrow N_2(X\ ^1\Sigma_g^+) + O(^3P) + 6.2\ \text{eV}, \quad (1a)$$

$$N_2(X\ ^1\Sigma_g^+) + O(^1D) + 4.2\ \text{eV}, \quad (1b)$$

$$N_2(X\ ^1\Sigma_g^+) + O(^1S) + 2.0\ \text{eV}, \quad (1c)$$

$$NO(X\ ^2\Pi) + N(^4S) + 2.9\ \text{eV}, \quad (1d)$$

$$NO(X\ ^2\Pi) + N(^2D) + 0.5\ \text{eV}. \quad (1e)$$

Reactions (1d) and (1e) may be major sources of NO and $N(^2D)$ in auroras and in the quiet daytime E region[1]; in addition, some of the exothermicity of these reactions may appear as vibrational energy in the product NO molecules. The further reaction of $N(^2D)$, formed in Reaction (1e), with ambient O_2 can also produce vibrationally excited NO.

The rate constant for quenching $N_2(A^3\Sigma_u^+)$ by oxygen atoms has been reported to be 2.2×10^{-11} [2] and 1.5×10^{-11} cm^3 molecule^{-1} s^{-1}.[3] However, Meyer *et al.*'s[2] number was measured relative to the rate constant for quenching $N_2(A)$ by molecular oxygen k_2, which they took to be 6.0×10^{-12} cm^3 molecule^{-1} s^{-1}, and should be reduced by a factor of 2 to conform to presently accepted values of k_2.[4] The determination of Dunn and Young[3] was made in a complicated system which could provide reactive species, in addition to $N_2(A)$, which might complicate the kinetics. Furthermore, their atomic oxygen number densities were subject to substantial uncertainties. Some aeronomic estimates[1] have favored a value closer to 10^{-10} cm^3 molecule^{-1} s^{-1}, although recent rocket measurements by Sharp *et al.*[5,6] and O'Neil *et al.*[7] are in conflict on this. Sharp *et al.*[5,6] favor a value of 2×10^{-10} cm^3 molecule^{-1} s^{-1}, while O'Neil *et al.*[7] support the earlier laboratory measurements with an estimate for k_1 of $(2-4)\times10^{-11}$ cm^3 molecule^{-1} s^{-1}.

Only Meyer *et al.*[2,8] have investigated the products of the reaction between $N_2(A)$ and oxygen atoms. They observed excitation of $O(^1S)$ by its characteristic emission at 557.7 nm, and estimated that $25^{+25}_{-10}\%$ of the total $N_2(A)$ quenching by oxygen atoms occurs via this path. This estimate is probably a lower limit since they neglected quenching of $O(^1S)$, which can be considerable in systems containing discharged oxygen. Our recent observations indicate a value much larger than this.[9] Their system was not sufficiently free from extraneous NO contamination to rule out the possibility of NO product formation as well.

During the course of a program to study product formation in Reaction (1), we remeasured the rate constants at 300 K for this reaction for both vibrational levels 0 and 1. Our results are about a factor of 2 higher than the corrected measurement of Meyer *et al.*[2] and that of Dunn and Young,[3] but a factor of 7 less than the aeronomic estimate of Sharp *et al.*[5,6] In contrast to the quenching of $N_2(A)$ by O_2, where $k_2^{v=1}/k_2^{v=0} = 1.8$,[4] the quenching of $N_2(A)$ by atomic oxygen shows only a 20% enhancement of $k_1^{v=1}$ over $k_1^{v=0}$.

II. EXPERIMENTAL

A. Apparatus

The experiments were done in a discharge–flow apparatus with the $N_2(A)$ number densities monitored by spectroscopic observations of individual vibrational bands of the Vegard–Kaplan $N_2(A^3\Sigma_u^+ - X^1\Sigma_g^+)$ system of nitrogen. The reactor, which has been described in detail previously,[4,9(a)] is a 2 in. diameter quartz tube which is pumped by a Roots blower that is capable of producing linear flow velocities up to 8×10^3 cm s^{-1} at pressures of 1 Torr. A 0.5 m monochromator (Minuteman) is mounted upon a set of rails parallel to the flow tube. Spectral observations of the luminous gases in the flow tube, therefore, can be made as a function of linear distance along the tube by sliding the monochromator up and down on its rails. Distances are converted to reaction times by dividing by the flow velocity. Light intensities are measured photoelectrically using a thermoelectrically cooled EMI 9558QA photomultiplier and an an SSR 1105 photon-counting rate meter.

The metastable nitrogen molecules are produced in the reaction between metastable $Ar(^3P_{0,2})$ and molecular nitrogen.[10,11] This transfer results in the production of nearly equal populations of the $C\ ^3\Pi_u$ and $B\ ^3\Pi_g$ states of N_2[12] which quickly cascade radiatively to the metastable $A\ ^3\Sigma_u^+$ state. The metastable argon is produced

 0021-9606/81/182847-06$01.00

by flowing argon through a cold, hollow-cathode discharge operated at about 210 V and 3 mA. The argon was purified by flowing it through a trap filled with a 5 A molecular sieve and cooled with dry ice. Typically, the argon flow rate is ~1500 μmol s^{-1}, the nitrogen flow rate is ~250 μmol s^{-1}, and the flow tube pressure is about 1.3 Torr. Typical flow velocities ranged from 1100–1500 cm s^{-1}. These were obtained by throttling the Roots blower, or by shutting the blower off and using only the forepump on the flow tube.

Atomic oxygen was made by dissociating O_2 in a microwave discharge through a small amount of O_2 in helium (typical flows: 1 μmol s^{-1} of O_2 and 100 μmol s^{-1} of He). The oxygen atoms were injected into the flow tube through a 1 in. diameter loop fabricated from 2 mm o.d. polyethylene tubing. Number densities of atomic oxygen were determined using the air-afterglow technique,[13,14] which required the injection of NO through a second loop in the flow tube about 10 cm downstream from the oxygen injector.

The molecular oxygen was purified by pumping on liquid O_2 prior to expanding the middle portion of the liquid O_2 into a 5–1 storage bulb. The nitric oxide used in the O-number-density determinations was purified by slowly flowing NO through an ascarite trap, and then a trap at dry ice temperature prior to storage in a 5–1 bulb.

B. Determination of atomic oxygen number density

When atomic oxygen and nitric oxide are mixed, a continuum emission called the air afterglow is observed, which extends from 375 to beyond 3000 nm.[13–22] The intensity of this emission is directly proportional to the product of the number densities of atomic oxygen and nitric oxide, and independent of pressure of bath gas, at least at pressures above about 0.2 Torr. Thus, the emission intensity of the air afterglow is given by

$$I_{O/NO} = \kappa_\lambda [O][NO] , \tag{2}$$

where κ_λ is a calibration constant specific to the particular viewing geometry and incorporates such things as detection system efficiency, the size of the observation volume, and the absolute air-afterglow rate constant. κ is a function of wavelength both through the detection ststems' spectral response as well as through the wavelength variation of the air-afterglow rate constant. The calibration constant κ is determined experimentally by titrating atomic nitrogen with excess NO:

$$N + NO \rightarrow N_2 + O . \tag{3}$$

In the absence of added nitric oxide, N-atom recombination produces chemiluminescence from the nitrogen first-positive bands, the intensity of which is proportional to the square of the N-atom number density:

$$N + N + M \rightarrow N_2(B^3\Pi_g) , \tag{4}$$

$$N_2(B^3\Pi_g) \rightarrow N_2(A^3\Sigma_u^+) + h\nu \quad \text{(first positive bands)} . \tag{5}$$

Upon addition of NO, the first positive emission intensity decreases until such a point that the quantity of NO added balances the amount of N atoms initially in the flow. At this point, the end point of the NO titration,

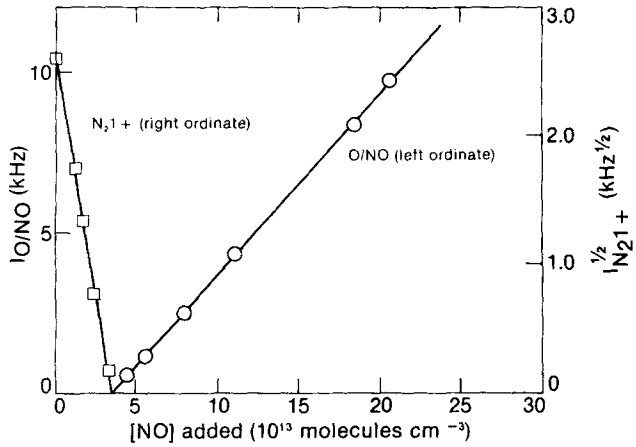

FIG. 1. Variation in emission at 580 ± 5 nm as a function of added [NO].

all N initially in the reactor has been quantitatively converted to O, and no emission is observed in the reactor. When even more NO is added to the reactor, the air-afterglow emission begins to be observed, and the intensity of the emission will vary linearly with the amount of NO added. An N-atom titration plot is shown in Fig. 1. The equation describing the change in the air-afterglow intensity as a function of added NO for NO additions beyond the titration end point is

$$I_{O/NO} = \kappa[O][NO] = \kappa[N]_0([NO]_0 - [N]_0) , \tag{6}$$

where κ is the constant of proportionality relating the air-afterglow intensity to the product [O][NO], $[N]_0$ is the number density of N atoms initially in the reactor prior to NO addition and the O-atom number density for NO additions beyond the titration end point, and $[NO]_0$ refers to the NO number density which would obtain in the absence of Reaction (3). The factor κ, then, is determined to be the ratio of the square of the slope to the intercept of the line describing the change in air-afterglow intensity with $[NO]_0$.[23]

O-atom number densities in the present experiments were determined by measuring the air-afterglow signal at 580 nm, with a 5 nm bandpass at at least three different NO number densities. Then [O] was taken to be the slope of the line representing the air-afterglow intensity as a function of [NO] divided by κ. Even through small amounts of ozone could be by-products of the O-atom discharge, there can be no interference from the O_3 + NO chemiluminescent reaction in the technique for determining the O-atom number density. The continuum generated from the O_3 + NO reaction has a short wavelength cutoff of 600 nm.[24]

A series of calibrations taken over a period of time established κ to ± 10%. The slopes of the $I_{O/NO}$ vs [NO] plots for the determination of [O] has standard deviations less than 5%. Thus, the determination of [O] is, in principle, accurate to ± 12%. Because the measurements of [O] were not made simultaneously with the kinetic measurements, it is possible that short-term variations in [O] could lead to differences between the number density of O measured and that actually in the reactor during the kinetic measurements. We shall

assume these differences to be random and therefore included in the experimental scatter in the data analysis.

C. Experimental technique for measurement of the quenching of $N_2(A)$ by atomic oxygen

Atomic oxygen is produced for the studies of the quenching of $N_2(A)$ by dissociating molecular oxygen in a microwave discharge of a trace of O_2 in helium. When the discharge is on, there are three important processes for $N_2(A)$ removal: deactivation at the wall (rate constant k_w), quenching by atomic oxygen (rate constant k_1), and quenching by molecular oxygen (rate constant k_2). With the discharge on, the equation describing the change in $N_2(A)$ number density with distance down the flow tube is given by

$$\bar{v} \ln \frac{[N_2(A)]^{on}}{[N_2(A)]_0} = (k_w + k_1[O] + k_2[O_2])z \ . \tag{7}$$

When the discharge is turned off, the $N_2(A)$ number density is given by

$$\bar{v} \ln \frac{[N_2(A)]^{off}}{[N_2(A)]_0} = -(k_w + k_2[O_2]_0)z \ . \tag{8}$$

When the discharge is on, the molecular oxygen number density is given by

$$[O_2] = [O_2]_0 - \tfrac{1}{2}[O] \ , \tag{9}$$

where $[O_2]_0$ is the number density of O_2 with the discharge off. Substituting Eq. (9) into Eq. (7) and taking the difference between Eqs. (7) and (8) results in an expression which relates the ratio of the $N_2(A)$ number density with the discharge on to that with it off to the rate constant of interest k_1, the atomic oxygen number density, and the reaction time, i.e.,

$$\bar{v} \ln \frac{[N_2(A)]^{on}}{[N_2(A)]_0} - \bar{v} \ln \frac{[N_2(A)]^{off}}{[N_2(A)]_0} = \bar{v} \ln \frac{[N_2(A)]^{on}}{[N_2(A)]^{off}} - (k_1 - \tfrac{1}{2}k_2)[O]z \ . \tag{10}$$

Plots of the left-hand side of Eq. (10) against [O] give lines whose slopes equal $(k_1 - \frac{1}{2}k_2)z = \Gamma'$. The slope from a plot of Γ' vs z can be used to obtain the unknown rate constant k_1 given the previously determined rate constant k_2.[4]

D. Flow analysis

In our apparatus there is essentially unit probability of $N_2(A)$ deactivation in collisions with the reactor walls. Thus, a radial gradient in $N_2(A)$ number density is set up in the flow tube, and this radial gradient, when coupled with a parabolic velocity profile resulting from laminar flow within the flow tube, affects the analysis of the rate constant measurements. The proper fluid dynamic analysis of this situation had been considered exhaustively in the literature.[25-32] In the ideal case, the parabolic velocity profile is fully developed, and the rate constants determined under the assumption of plug flow conditions must be multiplied by a factor of 1.6 to give the true rate constant. The time required for the development of a parabolic velocity profile in the reactor is usually translated into a traversal distance $z = 0.227aR$, where z is the distance from the inlet of the tube, a is the tube radius, and R is the Reynolds number of the flow. In our experiments R ranges from 35–55 and typical entry lengths vary from 20–32 cm. All our measurements were done 30–45 cm downstream of the reagent inlet, thus ensuring that the flow was fully developed even if there was some perturbation to the the flow from reagent addition.

III. RESULTS

Figures 2 and 3 show the plots of the left-hand side of Eq. (10) vs [O] for $N_2(A)$, $v' = 0$ at two different reaction distances, and Fig. 4 the plot of Γ' vs z for the $v' = 0$ measurements which monitored the 0, 6 Vegard–Kaplan band; Figs. 5, 6, and 7 show the similar plots for measurements made on the 1, 10 band. The slopes of the lines of Γ' vs z are $(1.7 \pm 0.1) \times 10^{-11}$ cm^3 molecule^{-1} s^{-1} for $v' = 0$ and $(2.0 \pm 0.1) \times 10^{-11}$ cm^3 molecule^{-1} s^{-1} for $v' = 1$, where the uncertainty given is one standard deviation in the least squres fit. The removal rate constants are then determined by multiplying these slopes by 1.6 to correct for flow effects (Sec. IID) and adding half of the rate constant for removal by molecular oxygen. We previously have determined these rate constants to be 2.3×10^{-12} and 4.1×10^{-12} cm^3 molecules^{-1} s^{-1} for $v' = 0$ and 1, respectively.[4] The final results for the removal of $N_2(A\,^3\Sigma_u^+)$ by atomic oxygen are $(2.8 \pm 0.2) \times 10^{-11}$ cm^3 molecule^{-1} s^{-1} for $v' = 0$ and $(3.4 \pm 0.2) \times 10^{-11}$ cm^3 molecule^{-1} s^{-1} for $v' = 1$. The total uncertainty (rms), including uncertainties in temperature, pressure, flow rate, O-atom number density, etc., is 15%

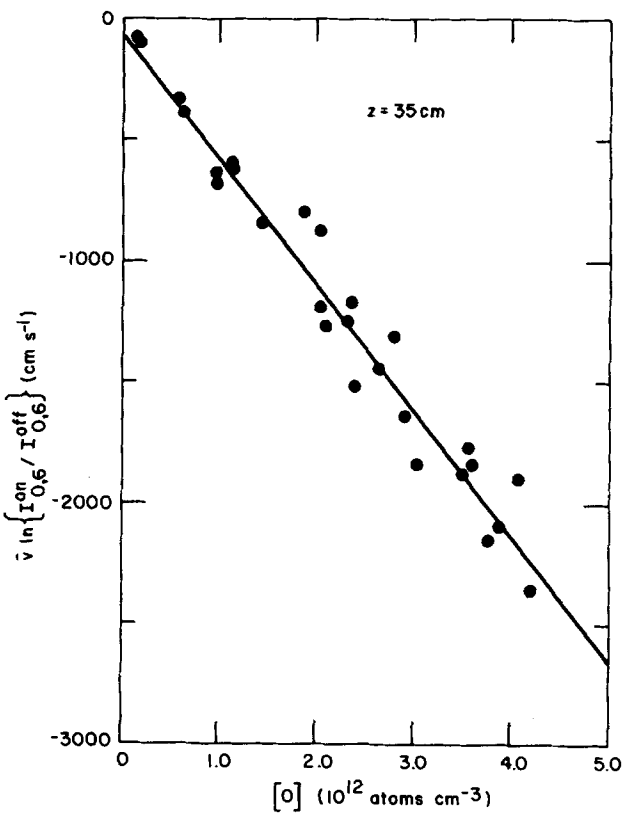

FIG. 2. The decay of $N_2(A)_{v=0}$ as a function of [O] for a mixing distance of 35 cm.

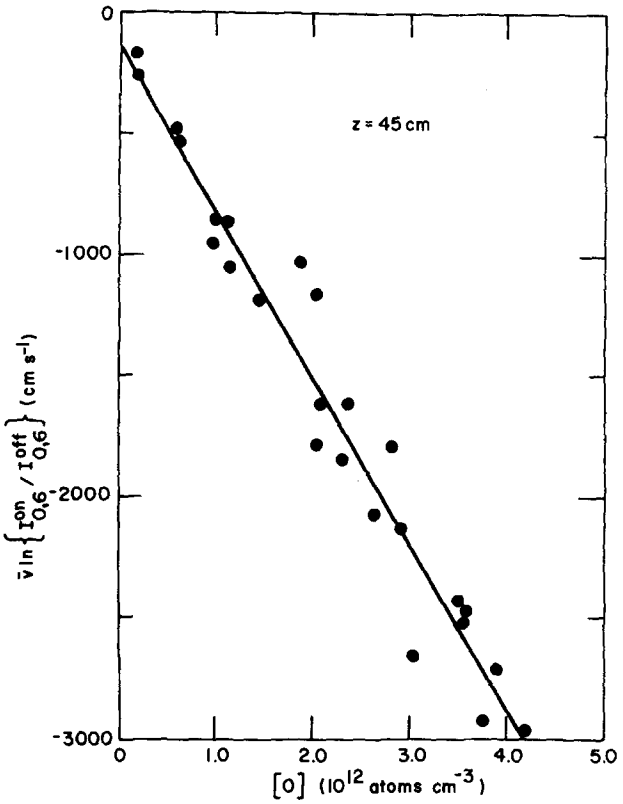

FIG. 3. The decay of $N_2(A)_{v=0}$ as a function of [O] for a mixing distance of 45 cm.

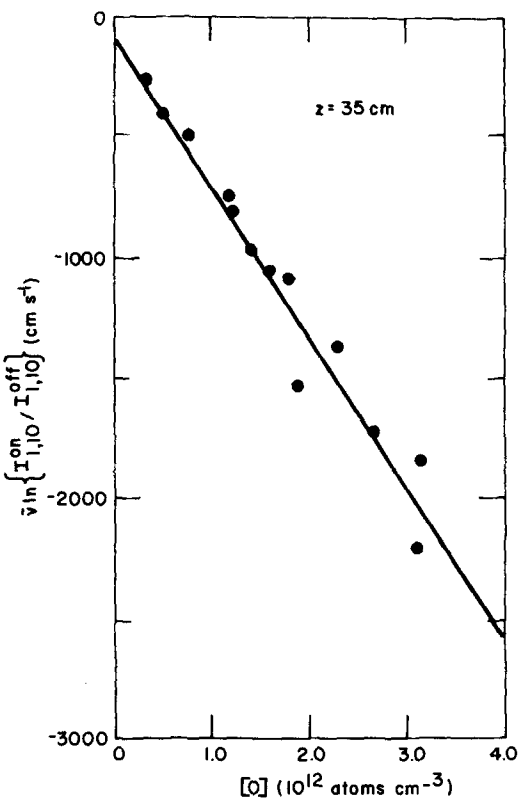

FIG. 5. The decay of $N_2(A)_{v=1}$ as a function of [O] for a mixing distance of 35 cm.

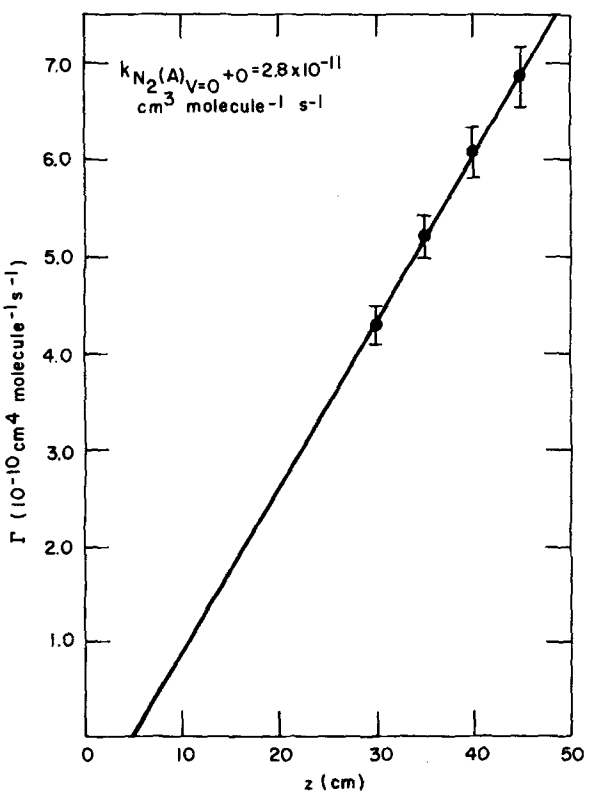

FIG. 4. Decay constants for $N_2(A)_{v=0} + O$ as a function of reaction distance.

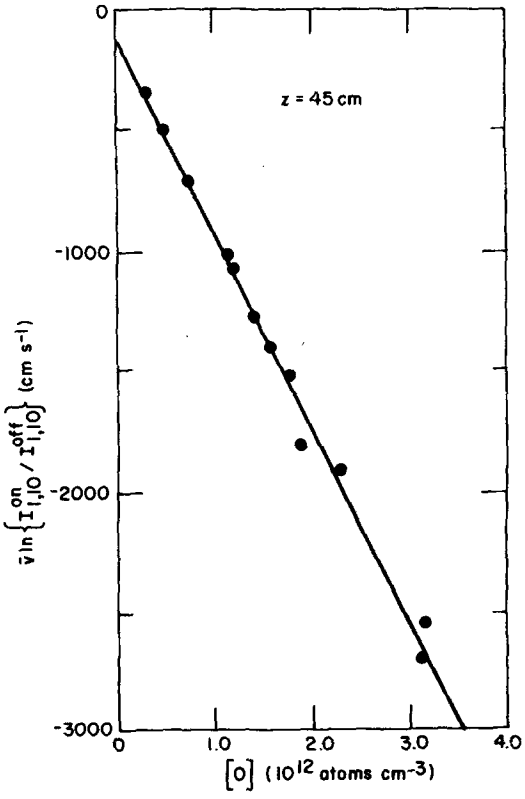

FIG. 6. The decay of $N_2(A)_{v=1}$ as a function of [O] for a mixing distance of 45 cm.

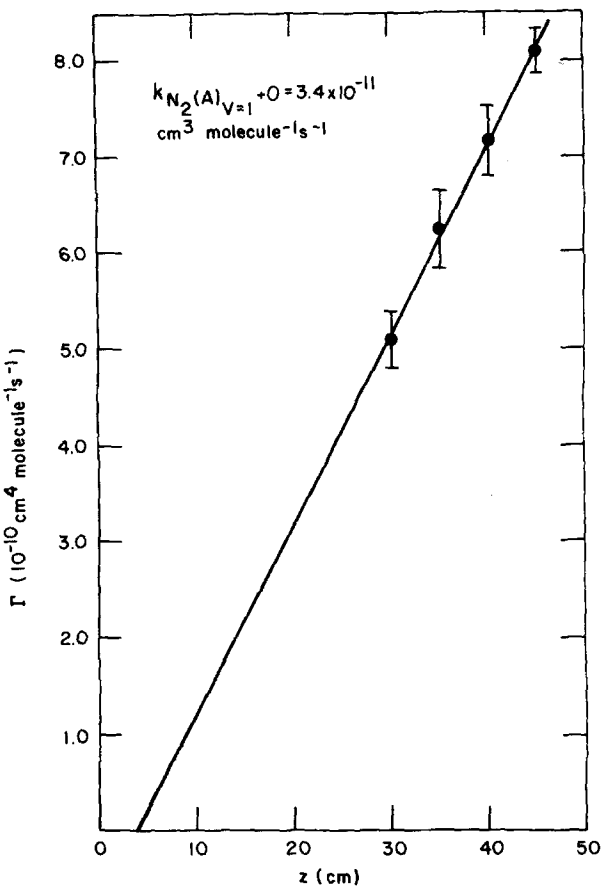

FIG. 7. Decay constants for $N_2(A)_{v=1} + O$ as a function of reaction distance.

for $v' = 0$ and 19% for $v' = 1$. These results are tabulated in Table I along with some other values which have appeared in the literature.

IV. DISCUSSION

At least two other species which are known to be produced to some extent in oxygen discharges also could be potential quenchers of $N_2(A)$. These species are ozone and $O_2(a\,^1\Delta)$. The electronically excited molecular oxygen is formed primarily through the heterogeneous recombination of atomic oxygen, while the ozone is formed from the three body reaction

$$O + O_2 + M \rightarrow O_3 + M$$

$$(k_{11} = 3.6 \times 10^{-34}\ \text{cm}^6\,\text{molecule}^{-2}\,\text{s}^{-1};\ \text{M} = \text{Ar}).^{33} \quad (11)$$

The ozone is destroyed by reaction with atomic oxygen

$$O + O_3 \rightarrow 2O_2$$

$$(k_{12} = 8.4 \times 10^{-15}\ \text{cm}^3\,\text{molecule}^{-1}\,\text{s}^{-1}),^{33} \quad (12)$$

reaction with $O_2(a\,^1\Delta)$,[34] and with hydrogeneous impurities in the discharged gas.[35] This latter removal process probably has the largest effect, but is the most difficult to assess. Given sufficient reaction time, Reactions (11) and (12) combine to give an upper limit to the steady-state concentration of O_3 which is governed by the ratio $k_{11}[M][O_2]/k_{12}$. We estimate that the pressure in the tube containing the atom discharge is about 7.8 Torr. Thus, the ratio $[O_3]/[O_2]$ ($\leq k_{11}[M]/k_{12}$) is less than or equal to 0.011, where we have made the assumption that the third body efficiency of helium in Reaction (11) is similar to that for argon. This assumption probably is good to ± 30%.[36]

The point of the above argument is that, in the worst case, the ozone number density in the reactor will be only 1% of the molecular oxygen number density, whereas the atomic oxygen number density is typically about 25% of the molecular oxygen number density. Thus, even if the rate constant for quenching $N_2(A)$ by ozone is 1×10^{-10} cm^3 molecule^{-1} s^{-1}, the measurement of the rate constant for quenching of $N_2(A)$ by O will be too large by only 12%. Given that our calculated ozone number density is an upper limit because of our neglect of the removal of ozone by $O_2(a\,^1\Delta)$ and by hydrogeneous impurities created in the discharge, we feel confident in rejecting ozone as a significant quencher of $N_2(A)$ in this series of measurements. However, the sidearm pressure was not varied to check for this effect.

Electronically excited molecular oxygen $O_2(a\,^1\Delta)$ could also be a potential quencher of $N_2(A)$. This species is produced to some extent in the discharge and also in the heterogeneous recombination of atomic oxygen of the Pyrex walls of the injector.[37] The presence of significant number densities of $O_2(a\,^1\Delta)$ in the gas stream can have two possible effects. If the electronically excited molecular oxygen quenches or reacts with $N_2(A)$ very efficiently, our rate constant for Reaction (1) will be too large. On the other hand, if the rate constant for the interaction between $N_2(A)$ and $O_2(a\,^1\Delta)$ is very small

TABLE I. Rate constants for removal of $N_2(A\,^3\Sigma_u^+)$ by O.

Rate constant[a]	Comments	Reference
2.2 (1.3)	Hg($6\,^3P$) tracer value from $k_O/k_{O_2} = 3$–4 and $k_{O_2} = 0.6 \times 10^{-11}$ cm^3 molecule^{-1} s^{-1}. Correcting to average value of k_{O_2} for 50/50 mixture of $N_2(A)$, $v = 0$ and 1 gives value in parentheses.	Meyer, Setser, and Stedman[2]
1.5	Looked at VK 0,6 and 1,5 with interference filters in pulsed $N_2/O_2/O$ discharge. Probably interference from NO γ bands. Substantial uncertainty in [O].	Dunn and Young[3]
2.8 ± 0.4 ($v = 0$) 3.4 ± 0.6 ($v = 1$)	Direct observation of decay of Vegard–Kaplan emission in discharge–flow reactor.	Present results
2–4	Estimate from rocket measurements of emissions in electron beam excited air at altitudes ≈ 100 km.	O'Neill, Lee, and Huppi[7]
20	Estimated from rocket measurements in an aurora.	Torr and Sharp[6]

[a]The listed rate constants are in units of 10^{-11} cm^3 molecule^{-1} × s^{-1} and are for $T = 300$ K.

($<10^{-13}$ cm^3 molecule^{-1} s^{-1}) and if, in addition, a large fraction of the undissociated molecular oxygen is in the $a\,^1\Delta$ state, then we will have overcorrected for quenching of $N_2(A)$ by the undissociated molecular oxygen, and the rate constant we present will be smaller than the true value. However, even if 100% of the undissociated molecular oxygen is in the $a\,^1\Delta$ state, our rate constant will be low by less than 25%.

Although we cannot think of mechanisms that would make $O_2(a\,^1\Delta)$ a significantly more efficient quencher of $N_2(A)$ than $O_2(X\,^3\Sigma^-)$, the combination of more than 30% of the undissociated O_2 in the $a\,^1\Delta$ state *and* an $N_2(A) + O_2(a\,^1\Delta)$ rate constant greater than 10^{-11} cm^3 molecule^{-1} s^{-1} would cause our measurement of k_1 to be high by more than 25%. As evidence that these two coincidental conditions did not obtain in the present experiments, we note that $O(^1S)$ is excited strongly in our reactor.[9] This excitation must be via Reaction (1c) because the dissociative excitation of $O_2(a\,^1\Delta)$ by $N_2(A)$ to make $O(^1S)$ and $O(^3P)$ is not energetically feasible. Preliminary results[9] indicate that most of the quenching of $N_2(A)$ by O leads to $O(^1S)$ excitation. Thus, the possible presence of $O_2(a\,^1\Delta)$ in our reactor cannot cause large errors in our measurements. Strictly speaking, however, our measurements should be considered upper limits until any effects of $O_2(a\,^1\Delta)$ on $N_2(A)$ quenching measurements can be demonstrated conclusively.

Our results, although of substantially improved accuracy, confirm the earlier laboratory measurements with respect to the order of magnitude of k_1. In addition, our values are in excellent agreement with the model-derived rate constants of O'Neil *et al.*[7] in their simulated-aurora, rocket experiments. The model-derived rate constant of Sharp *et al.*[5,6,38] of 2.0×10^{-10} cm^3 molecule^{-1} s^{-1} differs substantially from our measurements. The resolution of this discrepancy will require a careful reanalysis of the model and input data used by Sharp *et al.* to derive their rate constant.

ACKNOWLEDGMENTS

These experiments were conducted at the Air Force Geophysics Laboratories in Bedford, Mass. under AFOSR project No. 231064. PSI participation was funded under Air Force Contract #19628-77-C-0089. We are grateful for program support from both the Defense Nuclear Agency and the Air Force Office of Scientific Research. LGP appreciates interesting discussions with R. R. O'Neil (AFGL), T. G. Slanger (SRI, Int), E. A. Ogryzolo (University of British Columbia), and W. T. Rawlins (PSI).

[1]W. Swider, Geophys. Res. Lett. 3, 335 (1976).
[2]J. A. Meyer, D. W. Setser, and D. H. Stedman, J. Phys. Chem. 74, 2238 (1970).
[3]O. J. Dunn and R. A. Young, Int. J. Chem. Kinet. 8, 161 (1976).
[4]L. G. Piper, G. E. Caledonia, and J. P. Kennealy, J. Chem. Phys. 74, 2888 (1981).
[5]W. E. Sharp, M. H. Rees, and A. I. Stewart, J. Geophys. Res. 84, 1977 (1979).
[6]D. G. Torr and W. E. Sharp, Geophys. Res. Lett. 6, 860 (1979).
[7]R. R. O'Neil, E. T. P. Lee, and E. R. Huppi, J. Geophys. Res. 84, 823 (1979).
[8]J. A. Meyer, D. W. Setser, and D. H. Stedman, Astrophys. J. 157, 1923 (1969).
[9](a) G. E. Caledonia, L. G. Piper, W. T. Rawlins, and B. D. Green, PSI TR-233 (1980), available from the authors upon request; (b) L. G. Piper (manuscript in preparation).
[10]D. W. Setser, D. H. Stedman, and J. A. Coxon, J. Chem. Phys. 53, 1004 (1970).
[11]D. H. Stedman and D. W. Setser, Chem. Phys. Lett. 2, 542 (1968).
[12]J. H. Kolts, H. C. Brashears, and D. W. Setser, J. Chem. Phys. 67, 2931 (1977).
[13]F. Kaufman, Proc. R. Soc. London Ser. A 247, 123 (1958).
[14]F. Kaufman, *Chemiluminescence and Bioluminescence*, edited by M. J. Cormier, D. M. Hercules, and J. Lee (Plenum, New York, 1973), pp. 83–100.
[15]A. T. Stair and J. P. Kennealy, J. Chim. Phys. 64, 124 (1967).
[16]A. Fontijn, C. B. Meyer, and H. I. Schiff, J. Chem. Phys. 40, 64 (1964).
[17]M. Vanpee, K. D. Hill, and W. R. Kineyko, AIAA J. 9, 135 (1971).
[18]M. F. Golde, A. E. Roche, and F. Kaufman, J. Chem. Phys. 59, 3953 (1973).
[19]D. Golomb and J. H. Brown, J. Chem. Phys. 63, 5246 (1975).
[20]G. A. Woolsey, P. H. Lee, and W. D. Slafer, J. Chem. Phys. 67, 1220 (1977).
[21]M. Sutoh, Y. Morioka, and M. Nakamura, J. Chem. Phys. 72, 20 (1980).
[22]A. M. Pravilov and L. G. Smirnova, Kinet. Catal. (USSR) 19, 202 (1978).
[23]For a more complete discussion of this calibration process including caveats, please see Ref. 9(a).
[24]P. N. Clough and B. A. Thrush, Trans. Faraday Soc. 63, 915 (1967).
[25]E. E. Ferguson, F. C. Fehsenfeld, and A. L. Schmeltekopf, Adv. At. Mol. Phys. 5, 1 (1970).
[26]R. C. Bolden, R. S. Hemsworth, M. J. Shaw, and N. D. Twiddy, J. Phys. B 3, 45 (1970).
[27]A. L. Farragher, Trans. Faraday Soc. 66, 1411 (1970).
[28]R. W. Huggins and J. H. Cahn, J. Appl. Phys. 38, 180 (1967).
[29]R. E. Walker, Phys. Fluids 4, 1211 (1961).
[30]R. V. Poirier and R. W. Carr, J. Phys. Chem. 75, 1593 (1971).
[31]M. Cher and C. S. Hollingsworth, Adv. Chem. Ser. 80, 118 (1969).
[32]J. H. Kolts and D. W. Setser, J. Chem. Phys. 68, 4848 (1978).
[33]I. Arnold and F. J. Comes, Chem. Phys. 42, 231 (1979).
[34]K. H. Becker, W. Groth, and U. Schurath, Chem. Phys. Lett. 14, 489 (1972).
[35]J. L. McCrumb and F. Kaufman, J. Chem. Phys. 57, 1270 (1972).
[36]D. L. Baulch, D. D. Drysdale, J. Duxbury, and S. J. Grant, *Evaluated Kinetic Data for High Temperature Reactions* III: *Homogeous Gas Phase Reactions of the O_2–O_3 System, the CO–O_2–H_2 System and of Sulfur-containing Species* (Butterworths, London, 1976).
[37]G. Black and T. G. Slanger, J. Chem. Phys. 74, 6517 (1981).
[38]W. E. Sharp and D. G. Torr, J. Geophys. Res. 84, 5345 (1979).